Alignment of Inertial Navigators in Low-Speed Vehicles

HERBERT J. SANDBERG,* ARTHUR GELB,† AND ALAN L. FRIEDMAN‡
Dynamics Research Corporation, Stoneham, Mass.

This paper is addressed to some aspects of low-speed inertial system alignment. Particular attention is paid to practical problems encountered which limit the accuracy of alignment. The system under study has been taken to be of the three-gimbal north-vertical configuration (z-axis vertical, x-axis north, and y-axis east), including appropriate damping and gyrocompassing means. The earth is assumed spherical. Errors in indication of the vertical and azimuth due to both component random errors and vehicle motion are treated. It is noted that, in the analysis of system response due to vehicle motions, sinusoidal test excitations although analytically convenient are not generally a valid description of the true base motions of the vehicle. In fact, it is demonstrated that such sinusoidal testing leads to overly optimistic expectation of system errors. Vehicle motions instead are described in terms of an acceleration spectral density that is peaked at some nonzero angular frequency and that contains no energy at zero frequency. This represents an attempt to account for vehicle motion more realistically. It is graphically demonstrated that, since the inertial system behaves as a low-pass filter to the hypothesized acceleration random process, longer system settling times lead to lower rms navigation errors.

Introduction

THE specific alignment problem under consideration consists of choosing Schuler loop damping and system gyrocompass action in order to place a three-gimbal north-vertical platform in a prescribed orientation as rapidly as possible under the constraints of maximum allowable error at the vertical and azimuth indicating stations around the inertial navigator loop. Platform alignment can be accomplished automatically by inserting servo loops into the mechanization during the alignment period. In the north-vertical system under consideration the three gyros and two accelerometers are mounted on the same gimbaled platform (Fig. 1). Call θ_x,θ_y, and θ_z small angular errors in the orientation of the indicated (x,y,z) coordinate frame relative to the true coordinate frame. Thus, in the alignment procedure, an attempt is made to reduce θ_x,θ_y, and θ_z to minimal values within time to align requirements. It is noted that the inertial system alignment dynamics about the platform z and y axes are tightly coupled due to earth rotation but that alignment about x is almost independent of alignment about y and z. Also, alignment about x involves no gyrocompassing, merely seeking the vertical. Thus the x-axis (longitude) loop and the y- and z-axis (gyrocompass) loop can be considered to be uncoupled for small θ_x,θ_y, and θ_z.

The error sources are taken as gyro drift, speed source noise, and vehicle motions (in the absence of a speed source). Gyro drift is characterized as containing bias and random terms where the power spectral density of the random terms attains significant amplitude only in a frequency band that is well below the system bandwidth. Speed source noise is modeled as consisting of a bias and white noise term. The white noise term may, in fact, be band limited. In this paper, it is required only that its bandwidth be substantially larger than that of the inertial system. Two types of acceleration disturbing motions to the vehicle are considered. These are characterized as pure sinusoidal[1] and a band-limited acceleration spectrum with 0 d.c. energy. In this paper, only the system errors due to *random* component errors and vehicle motions are considered, since the bias error sources have been covered in Ref. 2.

Received by ARS July 19, 1962; revision received July 9, 1963.
* System Engineer. Member AIAA.
† Manager, System Analysis. Member AIAA.
‡ Vice President, Systems.

Dynamic Characteristics

Figure 2 illustrates the *error* block diagram for a gyrocompassing and vertical inertial navigation system. The system errors of interest are

θ_x,θ_y = vertical errors
θ_z = azimuth error
δL = latitude error
$\delta\lambda$ = longitude error
$\delta V_x,\delta V_y$ = velocity errors

S_1 and S_4 are gain constants for the velocity servo loops. S_2 and S_5 are to reduce the effective radius of the earth, R, and hence quicken the response of the system. S_3 is used to correct misorientation in azimuth. The S_i must, of course, be chosen such that the system remains stable while meeting the remaining desired performance characteristics. ϵ_i and ϵ_{vi} are the errors in the ith gyro and external velocity vector, respectively.

The longitude loop is second order, and hence no absolute stability problem is present. In the gyrocompass loop the problem breaks down to an analysis of a third-order servo

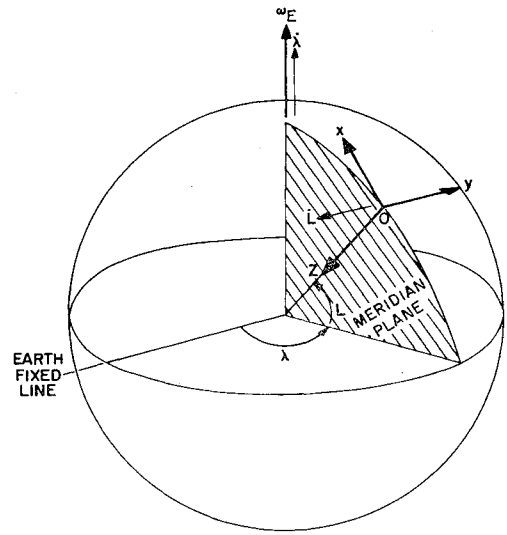

Fig. 1 Accelerometer and gyro (x,y,z) coordinate frame.

system with three variable parameters, S_1,S_2,S_3, subject to the criterion that, for stability (ω_E = earth rate),

$$S_1S_2 > S_3\omega_E \cos L \tag{1}$$

The gains S_1 to S_5 will be defined to yield second- and third-order loops with real and complex pole decay factors all equal. This leads to a "critically damped" third-order step response.[3] Following this procedure, it is seen that the characteristic equation of the gyrocompass loop[6,9] ($S_2 \gg 1$)

$$\Delta_1 = p^3 + p^2S_1 + p(g/R)S_2 + S_3(g/R)\omega_E \cos L \tag{2}$$

now takes the form

$$\Delta_1 = p^3 + p^2 3\zeta_n\omega_n + p\omega_n^2(1 + 2\zeta_n^2) + \zeta_n\omega_n^3 \tag{3}$$

where ζ_n is the gyrocompass loop damping ratio, ω_n is the gyrocompass loop natural frequency in radians per minute, and

$$\begin{aligned} S_1 &= 3\zeta_n\omega_n \\ S_2 &= (R/g)\omega_n^2(1 + 2\zeta_n^2) \\ S_3 &= (R/g)\cdot(1/\omega_E \cos L)\zeta_n\omega_n^3 \end{aligned} \tag{4}$$

The characteristic equation of the longitude loop[9] ($S_5 \gg 1$)

$$\Delta_2 = p^2 + pS_4 + g/R\, S_5 \tag{5}$$

now becomes

$$\Delta_2 = p^2 + 2\zeta_m\omega_m p + \omega_m^2 \tag{6}$$

where ζ_m is the longitude loop damping ratio, ω_m is the longitude loop natural frequency in radians per minute, and

$$\begin{aligned} S_4 &= 2\zeta_m\omega_m \\ S_5 &= (R/g)\omega_m^2 \end{aligned} \tag{7}$$

Using these dynamic relationships, the system response to random component errors and both sinusoidal and stochastic vehicle motions can be investigated.

Given the dynamic relationship just derived, the settling times of the second- and third-order loops of the inertial navigation system have been specified literally. As is customary, settling time T_s is defined as that time beyond which the transient response is bounded by $\pm 5\%$ of its final value following a step input. This is about three dominant system time constants given approximately by $3/\zeta$ for low ζ and 6ζ for high ζ. Figure 3 shows curves of dimensionless settling time ($\omega_{n,m}T_s$) vs system damping ratio ($\zeta_{n,m}$) for both loops of the analytically decoupled inertial system. The curves for the second- and third-order loops have been published elsewhere.[4, 8] It is seen that in each case there is a minimum settling time for a given system damping ratio.

Effect of Component Random Errors

The component random errors that are considered in this section are gyro drift and speed source error. (The speed source may be electromagnetic speed log, doppler radar, doppler sonar, etc.)

It is well known that a useful theoretical model for random gyro drift has an autocorrelation function given by

$$\varphi_{gg}(\tau) = A^2e^{-\beta|\tau|} \text{ (deg/hr)}^2 \tag{8}$$

where β is the inverse correlation time, and A^2 is the mean-squared value of gyro drift. The spectral density associated with Eq. (8) is

$$\Phi_{gg}(\omega) = (A^2/\pi)[\beta/(\beta^2 + \omega^2)]\text{(deg/hr)}^2\text{-hr} \tag{9}$$

Assume that the gyro correlation time β^{-1} is in the vicinity of 2 to 5 hr. Thus the gyro drift rate frequency spectrum lies well within the inertial system bandpass. Hence it is concluded that to a first-order the system passes the gyro drift, i.e., the system tracks the gyro drift perfectly.

Because of the nature of speed source implementation, the random component of the error is assumed to look "white"

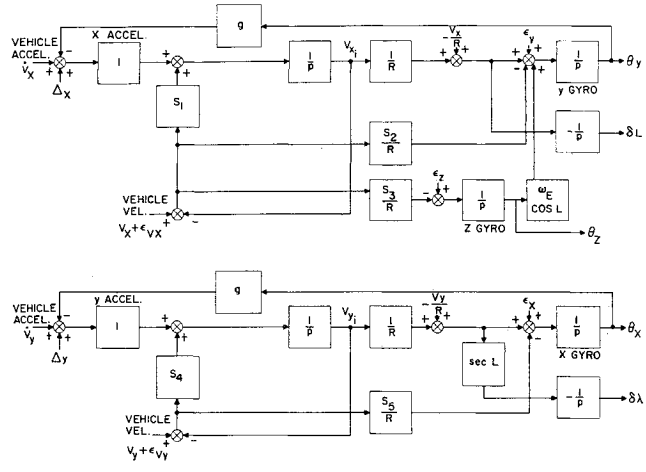

Fig. 2 Error block diagram of gyrocompassing and vertical system.

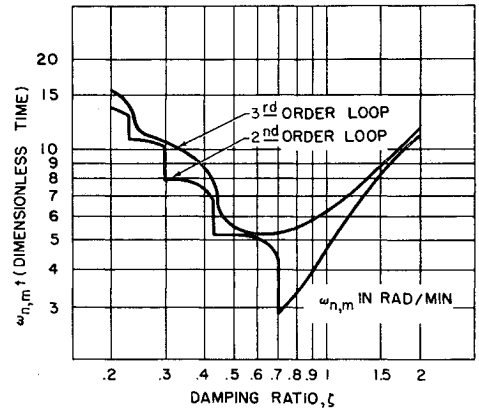

Fig. 3 Dimensionless settling time vs system damping ratio for gyrocompassing (third-order) and vertical (second-order) loops.

over the bandpass of the inertial system. Note that the actual error spectral density may itself be band limited; it merely is expected that the bandwidth of the noise is substantially larger than the inertial system bandwidth. To demonstrate this approximation in a limiting manner, the autocorrelation of the speed source error is defined to be

$$\varphi_{ss}(\tau) = D^2e^{-\gamma|\tau|} \text{ knots}^2 \tag{10}$$

which results in a power spectral density of the form

$$\Phi_{ss}(\omega) = (D^2/\pi)[\gamma/(\gamma^2 + \omega^2)] \text{ knots}^2\text{-time} \tag{11}$$

Now let $\gamma \to \infty$, so as to generate an impulse autocorrelation function

$$\Phi_{ss}(\omega) \to (1/\pi)[D^2/\gamma] \text{ knots}^2\text{-time} \tag{12}$$

where γ may actually be of the order of 100 to 1000/hr. If the white noise spectral density is defined by S_0, it follows that

$$S_0 = D^2/\gamma \text{ knots}^2\text{-time} \tag{13}$$

The steady-state ($t > 3/\zeta_{n,m}\omega_{n,m}$) rms vertical and azimuth errors due to uncorrelated random gyro drift and speed source error become (see Ref. 5 for the frequency domain calculation of mean-squared quantities)

$$[\langle\theta_x^2\rangle]^{1/2} = \left[\langle\epsilon_x^2\rangle\frac{4\zeta_m^2}{\omega_m^2} + S_{0y}\frac{[\omega_m^4 + (2\zeta_m\, g/R)^2]}{4\zeta_m\omega_m g^2}\right]^{1/2} \text{rad} \tag{14}$$

$$[\langle\theta_y^2\rangle]^{1/2} = \left[\langle\epsilon_z^2\rangle\frac{9\omega_E^2\cos^2 L}{\omega_n^4} + S_{0x} \times \frac{[\omega_n^4(1 + 6\zeta_n^2 + 12\zeta_n^4 + 8\zeta_n^6) + \zeta_n(\omega_n^2 - 3g/R)^2]}{g^2 4\zeta_n\omega_n(1 + 3\zeta_n^2)}\right]^{1/2} \text{rad} \tag{15}$$

$$[\langle\theta_z^2\rangle]^{1/2} = \left[\frac{\langle\epsilon_y^2\rangle}{\omega_E^2\cos^2 L} + \frac{\langle\epsilon_z^2\rangle(1+2\zeta_n^2)^2}{(\zeta_n\omega_n)^2} + S_{0x}\frac{\zeta_n\omega_n[(\omega_n^2 - g/R)^2 + 2\zeta_n\omega_n^4]}{4g^2\omega_E^2\cos^2 L(1+3\zeta_n^2)}\right]^{1/2} \text{rad} \quad (16)$$

where

$\langle\epsilon_x^2\rangle,\langle\epsilon_y^2\rangle,\langle\epsilon_z^2\rangle$ = mean-squared value of x,y, and z gyro drift, respectively
S_{0x},S_{0y} = values of x and y white noise speed source error spectral densities, respectively
ω_E = earth rate = 0.262 rad/hr

Note that for very lightly damped loops the speed source becomes the fundamental contributor to vertical errors, whereas z-gyro random drift dominates the azimuth error picture.

In a similar manner the rms errors in velocity may be computed. However, for the random processes described, the steady-state errors in latitude and longitude are unbounded, since they generate through an open-loop integration (see Fig. 2). These grow as $(t)^{1/2}$ for large t.

From Eq. (16), it is seen that the rms value of θ_z is inversely proportional to cos$L$. For navigation at low latitude, $[\langle\theta_z^2\rangle]^{1/2}$ may be within acceptable bounds, but as L approaches 90°, $[\langle\theta_z^2\rangle]^{1/2}$ is unbounded. Thus the gyrocompassing technique cannot be used near the polar regions because of the presence of component random errors.

Vehicle Motion Induced System Errors

This section is devoted to the self-damped inertial system. The inclusion of an external speed source would theoretically relieve this system of error dependence on vehicle motions, provided that the speed source and the inertial system are located at the same point in space.[7]

To obtain the effect on navigational system *errors* of any vehicle motions, the true velocity of the vehicle V_T must be appropriately disregarded. Figure 2 shows that acceleration of the vehicle, $\dot{V}$, is sensed and resolved by the x and y accelerometers. The resultant signals are integrated and divided by R to give indicated angular velocity signals V_i/R, which then act as electric inputs to the x and y gyros. To maintain the platform on the vertical as the vehicle navigates, the platform must be rotated with respect to inertial space at an angular rate V_T/R. The error in the indicated vertical is the integral of the error in the gyro-torquing rate, i.e.,

$$\int_0^t \left(\frac{V_i}{R} - \frac{V_T}{R}\right) dt$$

It can be shown that the system response at θ_x,θ_y, and θ_z to vehicle motions is affected only trivially by insertion of the term $-(V_T/R)$; however, for the error response at velocity, latitude, and longitude, the true vehicle angular velocity must be subtracted in order to obtain only the system *error* response, since this term is now nonnegligible. A convenient artifice for calculation in either instance is to hypothesize, for this self-damped system, a corresponding velocity-aided inertial system where the instantaneous speed source noise is equal and opposite in sign to the true vehicle velocity. This phantom speed source has as a result no output, yielding the required topological equivalence. All that need be done in this configuration is to insert $-V_T$ at the speed source input stations (in place of ϵ_{vx} and ϵ_{vy}) and observe vehicle errors as if the true acceleration and velocity were inserted at the input acceleration and indicated velocity levels, respectively. Such a maneuver is merely a computational device and has no real physical significance other than that already mentioned.

Independent of the navigating vehicle type, an inertial system will be subjected to spurious acceleration inputs that are the result of environmental influences, e.g., wind gusts. These must be studied in order to determine the trade-off point between the resultant system steady-state forced errors and the time to align. Call V_x and V_y the spurious (contaminating) north and east accelerations. The transfer functions relating vertical and azimuth errors to vehicle motions are as follows:

$$\frac{\theta_z}{\dot{V}_{x/g}} = p\frac{\zeta_n\omega_n^3}{\omega_E\cos L}\cdot\frac{1}{\Delta_1} \quad (17)$$

$$\frac{\theta_y}{\dot{V}_{x/g}} = \frac{p\omega_n^2(1+2\zeta_n^2) + \zeta_n\omega_n^3}{\Delta_1} \quad (18)$$

$$\frac{\theta_x}{\dot{V}_{y/g}} = \frac{\omega_m^2}{\Delta_2} \quad (19)$$

where $\dot{V}_x$ and $\dot{V}_y$ have the units of g's.

The system disturbing motions are described by a peaked acceleration frequency spectrum with zero energy at direct current. The response to such vehicle motions can be duplicated by putting white noise through an appropriate shaping filter and observing the mean-squared system outputs. The disturbing motions are assumed to be stationary in time, and the spectral density is defined such that the mean-squared value of normalized vehicle motions is unity, independent of the frequency characteristics of the filter.

The chosen spectral density is

$$|G(\omega)|^2 = \frac{4\zeta_1\omega_1\omega^2}{(\omega_1^2 - \omega^2)^2 + 4\zeta_1^2\omega_1^2\omega^2} \quad (20)$$

resulting from a shaping filter transfer function of the form

$$G(p) = \frac{2(\zeta_1\omega_1)^{1/2}p}{p^2 + 2\zeta_1\omega_1 p + \omega_1^2} \quad (21)$$

where ζ_1 is the shaping filter damping ratio, and ω_1 is the shaping filter natural frequency.

The vehicle motions, on the other hand, may be considered to be sinusoidal, of the form

$$\dot{V}_x = |\dot{V}_x|\sin\omega_s t \qquad \dot{V}_y = |\dot{V}_y|\sin\omega_s t \quad (22)$$

Assume

$$\omega_s = \omega_1 = 60 \text{ rad/min} \qquad \zeta_1 = 0.1$$
$$|\dot{V}_x| = |\dot{V}_y| = 0.01\,(2)^{1/2}g \quad (23)$$

and rms noise acceleration values of $0.01g$, so that the sinusoidal and random input acceleration rms values are identical. On the basis of the settling time curve (Fig. 3), one might choose $\zeta_n \approx 0.6$ in the gyrocompass loop and $\zeta_m \approx 0.8$ in the longitude loop. From Fig. 3 it is seen that, if $\zeta_n \approx 0.6$, then $t_n \approx 5.5/\omega_n$, and, correspondingly $\zeta_m \approx 0.8$ yields $t_m \approx 3.5/\omega_m$.

The effect of varying ω_n and ω_m on the rms errors in the vertical and azimuth as a function of system settling time is investigated now. Figures 4–6 show rms θ_z,θ_y, and θ_x, respectively, as a function of settling time for a range of system frequencies for both stochastic and sinusoidal inputs. Both ω_n and ω_m vary between 0.6 and 6.0 rad/min. As an example, assume that $\omega_m = \omega_n = 0.8$ rad/min. For stochastic inputs, it then follows that

$$\begin{aligned}\text{rms } \theta_z &= 6.2\times10^{-4}\sec L \text{ rad} \approx 120\sec L(\text{sec})\\ \text{rms } \theta_y &= 1.02\times10^{-5}\text{ rad} \approx 2.00(\text{sec})\\ \text{rms } \theta_x &= 5.7\times10^{-6}\text{ rad} \approx 1.10(\text{sec})\end{aligned} \quad (24)$$

and for sinusoidal inputs

$$\begin{aligned}\text{rms } \theta_z &= 1.6\times10^{-4}\sec L \text{ rad} \approx 32\sec L(\text{sec})\\ \text{rms } \theta_y &= 2.6\times10^{-6}\text{ rad} \approx 0.52(\text{sec})\\ \text{rms } \theta_x &= 1.75\times10^{-6}\text{ rad} \approx 0.35\ (\text{sec})\end{aligned} \quad (25)$$

where 1×10^{-5} rad $\approx$ 2(sec), and the gyrocompass and vertical loops would be settled in 7 and 4.5 min, respectively. In this case, and in fact in all such cases, azimuth error is

better than an order of magnitude higher than either of the vertical errors. Again note that, because of the sec$L$ modifier on azimuth error, the gyrocompassing technique cannot be used near the polar regions.

Comparison of the responses of the system to sinusoidal and stochastic inputs indicate that in each case the sinusoidal excitation gives lower rms errors for all system frequencies. However, the disturbing motions will, in fact, usually not be perfectly sinusoidal but generally will be better described as belonging to a random process such as given by Eq. (20). Thus it is seen that, because of observed discrepancies in the system responses, a sinusoidal response test of the system is apt to lead to overly optimistic prediction of system errors.

Though certain parameters have been specified in Figs. 4–6, the result obtained is applicable over a complete range of parameters. The system acts as a low-pass filter to the noise source; thus, the longer the allowed system settling time, the lower the rms navigation errors due to vehicle disturbing motions.

This analysis has been directed at vertical and azimuth errors. However, the same type error curves can be derived for position and velocity errors. The trade-off between settling time and rms errors is quite similar at all stations around the inertial navigator loop.

As a last step, observe that, for the example cited, the gains of the servo loops to be inserted into the system mechanization during alignment are

$$\begin{aligned} S_1 &= 3\zeta_n\omega_n = 1.2 \text{ rad/min} \\ S_2 &= (R/g)\omega_n^2(1 + 2\zeta_n^2) = 173 \\ S_3 &= (R/g)\zeta_n\omega_n^3(1/\omega_E \cos L) = 10{,}600 \sec L \\ S_4 &= 2\zeta_m\omega_m = 1.28 \text{ rad/min} \\ S_5 &= (R/g)\omega_m^2 = 115 \end{aligned} \tag{26}$$

where

$$R/g = 180 \text{ min}^2/\text{rad}$$

Discussion of Results

An inertial guidance system can be aligned by gyrocompassing and seeking the vertical, using the system's own instruments, and involving no external equipment. System performance during this alignment is contaminated by component bias errors, component random errors, and disturbing vehicle motions (in the absence of external velocity information).

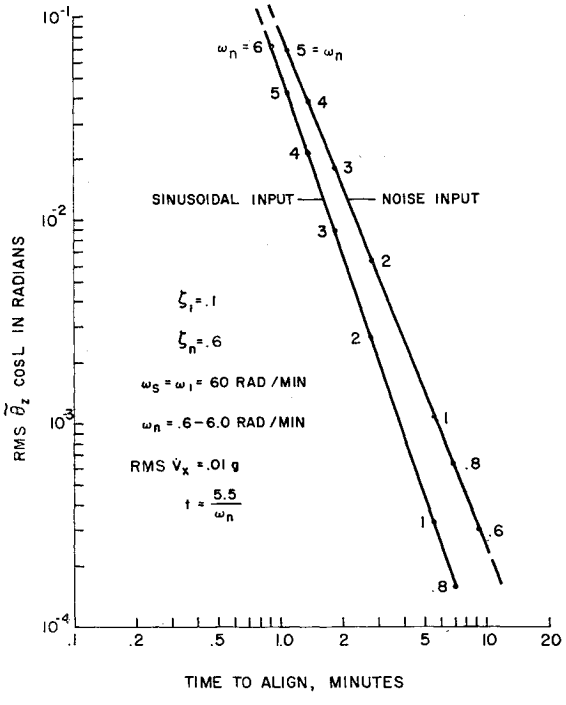

Fig. 4 Rms azimuth error vs time to align for various system natural frequencies.

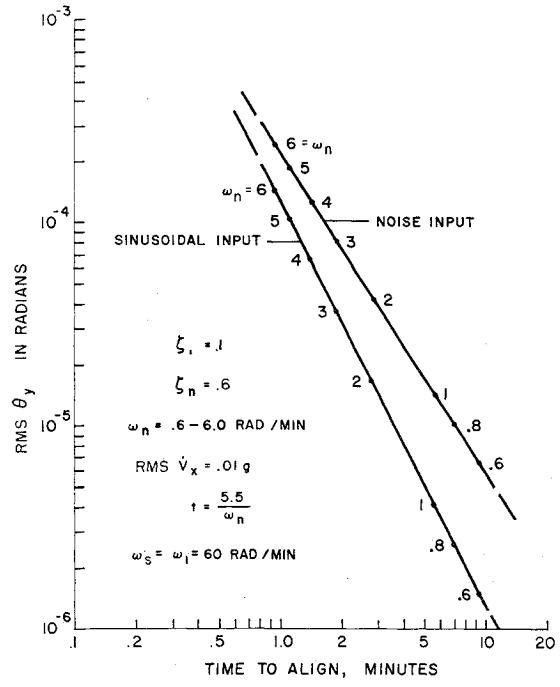

Fig. 5 Rms vertical error vs time to align for various system natural frequencies.

If rapid alignment is desired in the presence of disturbing base motions, then a trade-off must be made between alignment speed and resultant accuracy. In some instances it may be desirable to sacrifice some accuracy in the interest of rapid alignment. However, if alignment is to be performed on a moving base, in the absence of external speed information, base motions can be filtered only by lengthening the alignment time.

In the analysis of system response due to vehicle motions, it is shown that errors due to pure sinusoidal excitations give a low and relatively unrealistic prediction of the expected

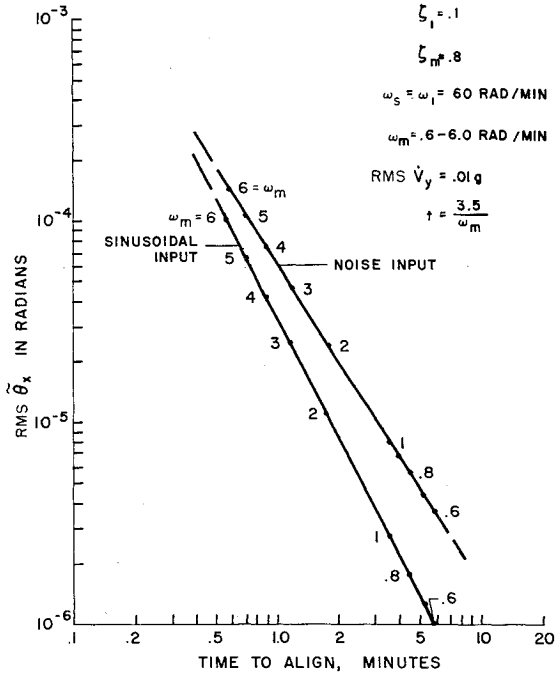

Fig. 6 Rms vertical error vs time to align for various system natural frequencies.

navigation rms errors. A better albeit higher mean-squared error prediction results from the use of a stochastic description for the vehicle acceleration.

References

[1] Cannon, R. H., Jr., "Alignment of inertial guidance systems by gyrocompassing—linear theory," J. Aerospace Sci. **28**, 885–895, 912 (1961).

[2] McMurray, L. R., "Alignment of an inertial autonavigator," ARS J. **31**, 356–360 (1961).

[3] Narendra, K. S., "Pole-zero configurations and transient response of linear systems," TR-299, Cruft Lab., Harvard Univ. (May 1959).

[4] Draper, C. S., McKay, W., and Lees, S., *Instrument Engineering* (McGraw-Hill Book Co. Inc., New York, 1953), Vol. 2, p. 265.

[5] Newton, G. C., Jr., Gould, L. A., and Kaiser, J. F., *Analytical Design of Linear Feedback Controls* (John Wiley and Sons, Inc., New York, 1957), Appendix E, pp. 366–381.

[6] Roitenberg, I. N., "The accelerated placing of a gyroscopic compass in a meridian," J. Appl. Math. Mech. **23**, no. 5, 1370–1374 (1959).

[7] Friedman, A. L., "The use of speed and position fix information in inertial navigators," ARS Preprint 1957-61 (August 1961).

[8] Gelb, A. and Sandberg, H. J., "Finding system settling time," Control Eng. **9**, 103–104 (November 1962).

[9] Pitman, G. R., Jr., *Inertial Guidance* (John Wiley and Sons, Inc., New York, 1962), Chap. 8, pp. 176–209.

SEPTEMBER 1963 AIAA JOURNAL VOL. 1, NO. 9

Optimum Transfers between Hyperbolic Asymptotes

FRANK W. GOBETZ*

United Aircraft Corporation, East Hartford, Conn.

An investigation was made to determine the possible benefits of a single high-thrust impulse during the hyperbolic encounter of a spacecraft with a perturbing planet. The equations are formulated to allow for the application of the method to any two- or three-dimensional hyperbolic transfer problem; thus, applications require knowledge only of the hyperbolic excess velocities and the total turning angle of the maneuver. For cases in which the planetary radius enforces a constraint on the closest approach distance, generalized charts are presented to indicate the attendant performance penalty that is imposed. In addition to the single-impulse transfers, a four-impulse maneuver is described. This maneuver has the advantage of reducing performance requirements as well as increasing the time spent in the vicinity of the planet.

Nomenclature

A,B,C	=	coefficients of quadratic equation [Eq. (A6)]
a	=	semimajor axis
F	=	prime focus; center of gravitational attraction
R	=	planet radius
r	=	length of radius vector
V	=	velocity
ΔV	=	characteristic velocity requirement of maneuver
α	=	angular change of velocity vector at impulse point
β	=	angle between incoming asymptotes
η	=	true anomaly
θ	=	path angle
κ	=	total turning angle of transfer maneuver
μ	=	gravitational parameter
ψ	=	complement of half angle of hyperbola (see Fig. 3)

Subscripts

a	=	approach
d	=	departure
p	=	closest approach
v	=	Venus
1	=	incoming hyperbola
2	=	outgoing hyperbola
∞	=	infinity relative to planet (sphere of influence)

Introduction

SEVERAL schemes have been advanced which use the perturbing effect of a celestial body to induce a velocity increment in a space vehicle. Lawden[1] has shown that about 50% of the heliocentric velocity changes required to effect Hohmann transfers to Venus and Mars can be obtained by perturbation maneuvers involving the Earth's moon. Crocco[2] has planned a 14-month round-trip interplanetary voyage to Venus and Mars during which propulsion is required only at Earth departure and Earth arrival. In this case, trajectory variations induced by close approaches to the planets allow the probe to rendezvous with Earth on the homebound leg of the trip. These two examples differ in one fundamental respect, namely, that in the first case the perturbation is sought deliberately, whereas in the second case it is inevitable. Nevertheless, in both cases the perturbation is used to good advantage.

In order to capitalize further on maneuvers of this type, it would be useful to investigate the possible benefits of applying thrust impulses during the hyperbolic encounter with a perturbing body. This problem has been considered previously in Ref. 3. In that study the optimum point for minimizing characteristic velocity was defined for single-impulse transfers, but no general numerical results were presented. Also, no allowance was made for a constraint on the closest approach distance during the encounter. Since such a constraint is a significant consideration, optimum solutions of the constrained problem are desirable. The purpose of this study was to extend the optimum solutions of Ref. 3 to constrained conditions and to examine the desirability of using a multi-impulse maneuver to effect the transfer.

Discussion of Problem

The general three-body problem can be well approximated (for space flight purposes) as a succession of two-body prob-

Presented at the AIAA Astrodynamics Conference, New Haven, Conn., August 19–21, 1963.

* Research Laboratories. Associate Member AIAA.